Title

Cellular cap-binding protein, eIF4E, promotes picornavirus genome restructuring and translation

Journal

Proceedings of the National Academy of Sciences of the United States of America, 114(36)

ISSN

0027-8424

Authors

Avanzino, Brian C
Fuchs, Gabriele
Fraser, Christopher S

Publication Date

2017-09-05

DOI

10.1073/pnas.1704390114

Peer reviewed

Cellular cap-binding protein, eIF4E, promotes picornavirus genome restructuring and translation

Brian C. Avanzino[a], Gabriele Fuchs[b,1], and Christopher S. Fraser[a,1]

[a]Department of Molecular and Cellular Biology, College of Biological Sciences, University of California, Davis, CA 95616; and [b]Department of Biological Sciences, The RNA Institute, University at Albany, State University of New York, Albany, NY 12222

Edited by Lynne E. Maquat, University of Rochester School of Medicine and Dentistry, Rochester, NY, and approved July 24, 2017 (received for review March 16, 2017)

Picornaviruses use internal ribosome entry sites (IRESs) to translate their genomes into protein. A typical feature of these IRESs is their ability to bind directly to the eukaryotic initiation factor (eIF) 4G component of the eIF4F cap-binding complex. Remarkably, the hepatitis A virus (HAV) IRES requires eIF4E for its translation, but no mechanism has been proposed to explain this. Here we demonstrate that eIF4E regulates HAV IRES-mediated translation by two distinct mechanisms. First, eIF4E binding to eIF4G generates a high-affinity binding conformation of the eIF4F complex for the IRES. Second, eIF4E binding to eIF4G strongly stimulates the rate of duplex unwinding by eIF4A on the IRES. Our data also reveal that eIF4E promotes eIF4F binding and increases the rate of restructuring of the poliovirus (PV) IRES. This provides a mechanism to explain why PV IRES-mediated translation is stimulated by eIF4E availability in nuclease-treated cell-free extracts. Using a PV replicon and purified virion RNA, we also show that eIF4E promotes the rate of eIF4G cleavage by the 2A protease. Finally, we show that cleavage of eIF4G by the poliovirus 2A protease generates a high-affinity IRES binding truncation of eIF4G that stimulates eIF4A duplex unwinding independently of eIF4E. Therefore, our data reveal how picornavirus IRESs use eIF4E-dependent and -independent mechanisms to promote their translation.

translation initiation | IRES | eIF4E | eIF4A | picornavirus

Cellular mRNAs use a cap-dependent mechanism for ribosome recruitment. This involves the binding of the 5′ 7-methylguanosine (m^7G) mRNA cap to the eIF4F complex, which consists of the cap-binding protein (eIF4E), a RNA-dependent DEAD box helicase (eIF4A), and the eIF4G scaffold protein. In contrast, picornaviruses use a cap-independent mechanism that uses an internal ribosome entry site (IRES) to bind directly to initiation factors (1, 2). The poliovirus (PV) and encephalomyocarditis virus (EMCV) IRESs are thought to require all canonical translation initiation factors except eIF4E (3–5). Importantly, specific domains near the 3′ borders of the PV and EMCV IRESs (domains V and J-K, respectively) provide binding sites for eIF4G (6–8). A key function of eIF4G is to recruit eIF4A so that its helicase activity can unwind RNA around the AUG initiation codon (6, 7). Consistent with this, picornavirus IRES-mediated translation is particularly sensitive to inhibition of eIF4A helicase activity (9, 10). However, little is known about how eIF4A helicase activity is controlled on IRESs.

Many picornaviruses inhibit host cell translation during infection to reduce an antiviral response and decrease competition between the viral and cellular mRNAs for translation components. Host translation is inhibited in PV infection by 2A protease ($2A^{pro}$) targeted cleavage of eIF4G (11, 12). Importantly, the PV IRES binds the C-terminal eIF4G cleavage product, enabling maintenance of efficient viral translation late in infection. Picornaviruses also reduce the availability of eIF4E and its ability to bind intact eIF4G through multiple mechanisms. Both EMCV and PV induce 4E-BP1 dephosphorylation to sequester eIF4E during the late stages of infection (13). In addition, eIF4E becomes localized to the nucleus during PV infection concomitant with eIF4G cleavage (14). Importantly, experimentally reducing eIF4E availability in cells promotes a switch from cap-dependent to IRES-mediated translation (5); however, reduced eIF4E availability also has been shown to decrease the rate of EMCV IRES-mediated translation, but only when endogenous mRNAs have been removed by nuclease treatment in cell-free extracts (3, 5). Therefore, eIF4E can have both positive and negative effects on the fundamental mechanism of picornavirus IRES-mediated translation. Interestingly, translation of the hepatitis A virus (HAV) is strongly dependent on eIF4E availability in cell-free extracts (15–17). This is surprising, given that the HAV genome, like all picornaviruses, does not have a 5′ m^7G cap. Although the negative role of eIF4E availability in IRES-mediated translation is consistent with an altered state of competition between cellular and viral mRNAs, no mechanism has been proposed to explain how eIF4E can stimulate IRES-mediated translation.

Here we used a nuclease-treated cell-free system to quantify the extent to which PV, HAV, and EMCV IRES-mediated translation is stimulated by eIF4E. We further show that eIF4E increases the translation rate of a PV replicon in this system. To provide a plausible molecular mechanism to explain these data, we used an IRES-dependent duplex unwinding assay to show that eIF4E controls IRES restructuring by promoting the helicase activity of eIF4A. This is due to an eIF4E-dependent increase in the rate of eIF4A duplex unwinding and an increase in the binding affinity of eIF4G for the PV and HAV IRESs. We also show that the cleavage of eIF4G by $2A^{pro}$ generates a high-affinity IRES-binding truncation that is able to efficiently restructure the PV and HAV IRESs independently of eIF4E. Consistent with previous data, we also show that eIF4E greatly stimulates the cleavage of eIF4G when $2A^{pro}$ is expressed and processed from a PV replicon. Thus, our data provide mechanistic insight into how eIF4E can play a positive role in IRES-mediated translation, and reveal an unexpected commonality in the mechanism

Significance

Picornaviruses translate their RNA genomes by a cap-independent mechanism that uses an internal ribosome entry site (IRES) to hijack the host translation machinery. The hepatitis A virus (HAV) and poliovirus (PV) IRESs contain binding sites for the eIF4G component of the cap-binding complex, eIF4F. The HAV IRES also requires eIF4E for efficient translation, but the reason for this is unknown. We now show that eIF4E increases the affinity of eIF4F for the HAV IRES and strongly stimulates the helicase activity of eIF4A. Remarkably, we show that PV IRES-mediated translation is also stimulated by eIF4E using the same mechanism of regulated eIF4F recruitment and helicase activity. This reveals an unexpected commonality in the mechanism that picornavirus IRESs use to recruit eIF4F.

Author contributions: B.C.A., G.F., and C.S.F. designed research; B.C.A. and G.F. performed research; B.C.A., G.F., and C.S.F. analyzed data; and B.C.A., G.F., and C.S.F. wrote the paper.

The authors declare no conflict of interest.

This article is a PNAS Direct Submission.

[1]To whom correspondence may be addressed. Email: gfuchs@albany.edu or csfraser@ucdavis.edu.

This article contains supporting information online at www.pnas.org/lookup/suppl/doi:10.1073/pnas.1704390114/-/DCSupplemental.

used by HAV and PV IRESs to recruit eIF4F and restructure their RNA domains.

Results

eIF4E Stimulates IRES-Mediated Translation in a Nuclease Treated Cell-Free Extract. To precisely establish the extent to which eIF4E availability can regulate cap-dependent and cap-independent IRES-mediated translation, we quantitatively manipulated eIF4E availability in a nuclease-treated rabbit reticulocyte lysate (RRL) cell-free extract system. We used three different reporters to monitor the following translation initiation mechanisms: (*i*) cap-dependent; (*ii*) HAV IRES-mediated; and (*iii*) PV IRES-mediated (Fig. 1*A*). The translation conditions were adjusted to ensure high-fidelity initiation codon selection (18). The RRL was also supplemented with HeLa cytoplasmic extract for all PV IRES translation experiments to ensure high-fidelity PV IRES-mediated translation (19), which was verified using a PV IRES mutant that lacks domain V (dV; *SI Appendix*, Fig. S1). Using this translation system, we first preincubated the lysate with increasing concentrations of purified recombinant 4E-BP1 to sequester the available eIF4E. Our data clearly reveal a dose-dependent inhibition of cap-dependent and both IRES-mediated translation mechanisms (Fig. 1 *B–D*). As expected, cap-dependent translation was severely inhibited by ≈80% at high 4E-BP1 concentrations (Fig. 1*B*). Unexpectedly, 4E-BP1 also inhibited both the HAV and PV IRES-mediated translation mechanisms by ≈40–50% (Fig. 1 *C* and *D*). Importantly, the inhibitory effect of 4E-BP1 on translation was specific and a direct effect of eIF4E sequestration, as incubating equimolar amounts of 4E-BP1 and eIF4E in the lysate did not inhibit translation compared with the control lysate (Fig. 1 *B–D*). In addition, translation directed by the unrelated HCV IRES, which does not require eIF4F, was insensitive to both recombinant 4E-BP1 and eIF4E addition (*SI Appendix*, Figs. S2*A* and S3*E*). We also found that the lysate was limiting for eIF4E, observing a 30–50% increase in cap-dependent, PV, and HAV IRES-mediated translation on addition of recombinant eIF4E (Fig. 1 *B–D* and *SI Appendix*, Fig. S3 *A–C*). Furthermore, we also found that the EMCV IRES and PV IRES behave similarly (Fig. 1*D* and *SI Appendix*, Fig. S2*B*). These data indicate that both cap-dependent and IRES-mediated translation mechanisms are regulated by eIF4E availability.

Cap-dependent and HAV IRES-mediated translation mechanisms are inhibited by cap analogs (15, 17). As expected, the addition of m^7GTP, but not of GDP, inhibited cap-dependent translation by 80% and HAV IRES-mediated translation by 60% in our lysate system (Fig. 1 *B* and *C*). In contrast, PV and EMCV IRES-mediated translation was not inhibited by either m^7GTP or GDP (Fig. 1*D* and *SI Appendix*, Fig. S2*B*), supporting the idea that eIF4E stimulates PV and EMCV IRES-mediated translation independent of its cap-binding function. Consistently, the addition of eIF4E with a W56L mutation to disrupt its cap-binding ability inhibits HAV IRES-mediated translation by ≈50%, but stimulates PV and EMCV IRES-mediated translation to a similar extent as wild-type eIF4E (*SI Appendix*, Fig. S4).

To determine whether intact eIF4G is required for stimulation of translation by eIF4E, we preincubated lysates with recombinant foot-and-mouth disease virus (FMDV) Lb protease, which cleaves eIF4G 7 aa upstream of the PV $2A^{pro}$ site (20). Consistent with previously published results (21), cleavage of eIF4G in the lysate by FMDV Lb protease stimulated PV translation by ≈2.5-fold (*SI Appendix*, Fig. S5). After cleavage of eIF4G, the addition of 4E-BP1 or eIF4E had no effect on PV translation (*SI Appendix*, Fig. S5*B*). Thus, our data suggest that IRES mechanisms that share a requirement for eIF4G/4A for translation also require eIF4E for efficient translation. This commonality is apparent even though PV and EMCV IRESs are classically considered eIF4E independent.

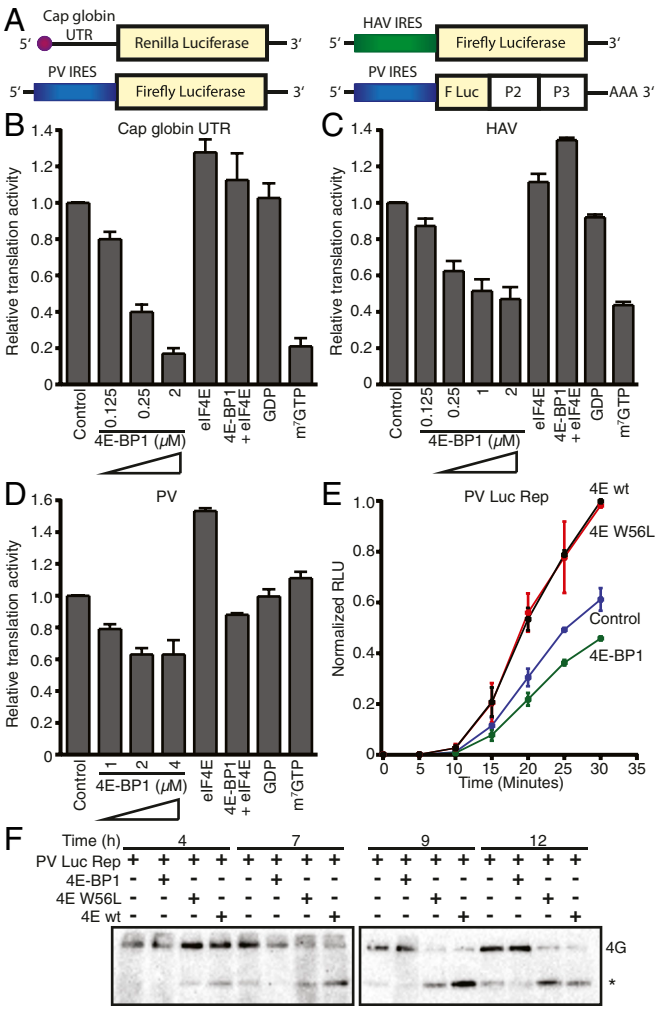

Fig. 1. eIF4E stimulates IRES-mediated translation and eIF4G cleavage in nuclease-treated extracts. (*A*) Schematic diagram depicting capped globin 5′ UTR, HAV, and PV IRES reporters as well as PV-Luc replicon. (*B*) Cap Rluc translation in the presence of indicated amounts of 4E-BP1, 1 μM eIF4E, equimolar eIF4E and 4E-BP1 (1 μM each), 20 μM GDP, or m^7GTP. (*C*) HAV Fluc translation in the presence of indicated amounts of 4E-BP1, 1 μM eIF4E, equimolar eIF4E and 4E-BP1 (1 μM each), 20 μM GDP, or m^7GTP. (*D*) PV-Fluc translation in the presence of indicated amounts of 4E-BP1, 1 μM eIF4E, equimolar eIF4E and 4E-BP1 (1 μM each), 20 μM GDP, or m^7GTP. (*E*) PV-Luc replicon translation in the presence of 2 μM eIF4E, eIF4E W56L, or 4E-BP1. (*F*) Immunoblot depicting cleavage of eIF4G in RRL supplemented with HeLa lysate in the presence of 2 μM 4E-BP1, eIF4E W56L, or eIF4E at the indicated times after addition of PV-Luc replicon RNA. Full-length eIF4G is indicated, and the asterisk denotes the eIF4G cleavage product. Data are the mean of at least three independent experiments, and error bars indicate SEM.

eIF4E Stimulates Translation of a PV Replicon and Viral-Mediated Cleavage of eIF4G. A limitation of the in vitro translation system is that reporter genes containing an IRES do not always faithfully recapitulate translational regulation facilitated by other portions of the mature mRNA. Other features of the genomic PV RNA, including the 3′ UTR and poly(A) tail, can influence translation (22–24). Therefore, we used a more physiologically relevant RNA, a PV replicon in which the P1 region of the PV genome is replaced with a firefly luciferase reporter. This PV-Luc replicon construct contains the viral genes necessary for replication, as well as the PV 3′ UTR and the poly(A) tail (25) (Fig. 1*A*). 4E-BP1 inhibited translation of the PV-Luc replicon by ≈25% after 30 min, and both eIF4E WT and eIF4E W56L stimulated PV-Luc

replicon translation by 60% (Fig. 1*E*). These results show that eIF4E stimulates translation of a replication-competent PV RNA.

Previous studies found eIF4E greatly stimulates cleavage of eIF4G in vitro using purified viral proteases (26, 27). Here we found that eIF4E greatly stimulated the rate of eIF4G cleavage from $2A^{pro}$ expressed and processed from the PV-Luc replicon (Fig. 1*F*). To verify that $2A^{pro}$ expressed from the PV-Luc replicon is fully functional, we repeated the experiment using RNA extracted from PV virions, and observed the same result (*SI Appendix*, Fig. S6*A*). Importantly, the eIF4E-mediated stimulation of eIF4G cleavage also occurred in HeLa lysate alone, albeit at a faster rate (*SI Appendix*, Fig. S6 *B* and *C*). These data demonstrate that functional protease expressed and processed from genomic PV RNA is dependent on eIF4E to efficiently cleave eIF4G.

eIF4E Stimulates eIF4A-Dependent Duplex Unwinding on the HAV and PV IRESs. Binding of human eIF4E to eIF4G promotes RNA restructuring by stimulating eIF4A helicase activity on a short RNA duplex with an unstructured loading strand (28). We generated an IRES-dependent restructuring assay by modifying our fluorescent helicase assay (29) to include either the HAV or PV IRES on the 5′ side of the fluorescent-labeled molecular beacon binding sites (Fig. 2*A*). This assay enables accurate real-time kinetic measurements of strand separation in the region located immediately after the authentic initiation codon of HAV (AUG_{735}) and PV (AUG_{743}). For our study, we used a previously characterized eIF4G truncation that contains the eIF4E-binding site and the C terminus of human eIF4G (28), $eIF4G_{557–1,599}$ (Fig. 2*B*). In the absence of eIF4E, the rate of duplex unwinding by eIF4A in the presence of eIF4B and $eIF4G_{557–1,599}$ was only moderately efficient on both HAV and PV IRESs (Fig. 2 *C* and *E* and *SI Appendix*, Table S1). Strikingly, the addition of eIF4E appreciably stimulated both the initial rate of duplex unwinding and the maximum amplitude of unwinding reactions on both IRESs (Fig. 2 *C–F* and *SI Appendix*, Table S1). The unwinding is eIF4A-dependent, given that the addition of 5 μM hippuristanol resulted in an ≈75% inhibition in the initial rate of duplex unwinding for reactions containing eIF4A, eIF4B, $eIF4G_{557–1,599}$, and eIF4E (*SI Appendix*, Fig. S7 *A–D*). We also found that eIF4A alone or in combination with eIF4B and eIF4E is a poor helicase on HAV and PV IRESs. Moreover, in the absence of eIF4A, a combination of eIF4E, eIF4B, and $eIF4G_{682–1,599}$ did not exhibit appreciable unwinding activity (*SI Appendix*, Fig. S7 *A–D*).

To determine whether the cap-binding function of eIF4E is required for the observed stimulation of eIF4A duplex unwinding activity, we repeated our unwinding assay in the presence of either m^7GTP or eIF4E W56L. The initial rate of HAV IRES duplex unwinding was similar when eIF4E was added in the absence or presence of m^7GTP or when eIF4E W56L was used (Fig. 2*D* and *SI Appendix*, Fig. S8*A* and Table S1). We also found that the rate of PV IRES-mediated duplex unwinding was stimulated to the same degree when eIF4E was added in the presence of m^7GTP or when eIF4E W56L was used (Fig. 2*F* and *SI Appendix*, Fig. S8*B* and Table S1). This strongly suggests that the unwinding activity of eIF4F on the HAV and PV IRESs in the presence of eIF4B is not dependent on the cap-binding function of eIF4E.

To determine whether eIF4G cleavage by $2A^{pro}$ regulates eIF4A-dependent duplex unwinding activity on the HAV and PV IRESs, we generated an eIF4G truncation mimicking the C-terminal fragment following $2A^{pro}$ cleavage ($eIF4G_{682–1,599}$; Fig. 2*B*). At a concentration approaching saturation (1 μM), $eIF4G_{682–1,599}$ stimulated eIF4A duplex unwinding activity on the HAV and PV IRESs to approximately the same degree as $eIF4G_{557–1,599}$ in the presence of eIF4E (Fig. 2 *C–F* and *SI Appendix*, Table S1). This demonstrates that cleavage of eIF4G by $2A^{pro}$ relieves the requirement of eIF4E for optimal unwinding activity on both IRESs. It also explains why eIF4E availability does not regulate IRES-mediated translation following eIF4G cleavage (*SI Appendix*, Fig. S5*B*). The direct interaction of eIF4G with the PV IRES has been mapped to dV (6). To verify that efficient PV IRES-mediated duplex unwinding requires the specific interaction between eIF4G and dV, we monitored the rate of duplex unwinding on a mutant PV IRES with dV deleted. We found a 50% reduction in the rate of unwinding by eIF4A in the presence of $eIF4G_{682–1,599}$ and eIF4B (Fig. 2*F* and *SI Appendix*, Fig. S7*E* and Table S1). This confirms that dV plays an important role in directing eIF4A-dependent restructuring of the PV IRES, and that our assay accurately monitors IRES-dependent duplex unwinding.

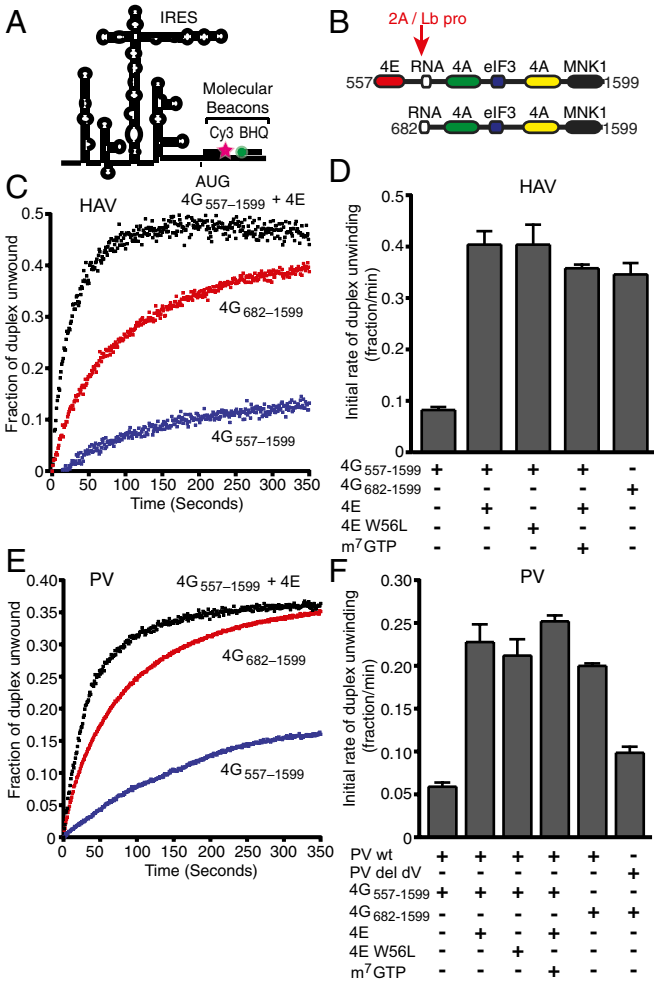

Fig. 2. eIF4E stimulates eIF4A duplex unwinding on the HAV and PV IRESs. (*A*) Schematic depicting the IRES construct with the Cy3 and BHQ molecular beacons used in the unwinding assay. (*B*) Cartoon depicting human eIF4G constructs used, with interaction domains and sites of 2A/Lb protease cleavage indicated. (*C*) Representative time course of unwinding reactions containing 50 nM HAV IRES RNA and 1 μM eIF4A, eIF4B, and $eIF4G_{557–1,599}$ in the absence (blue) or presence of eIF4E (black) or $eIF4G_{682–1,599}$ (red). (*D*) Initial rate of duplex unwinding of 50 nM HAV IRES RNA and 1 μM eIF4A, eIF4B, and the indicated proteins or 20 μM m^7GTP. (*E*) Representative time course of unwinding reactions containing 50 nM PV IRES RNA and 1 μM eIF4A, eIF4B, and $eIF4G_{557–1,599}$ in the absence (blue) or presence of eIF4E (black) or $eIF4G_{682–1,599}$ (red). (*F*) Initial rate of duplex unwinding of 50 nM of indicated PV IRES RNA and 1 μM eIF4A, eIF4B, and the indicated proteins or 20 μM m^7GTP.

eIF4E Increases the Affinity and Rate of IRES-Mediated Duplex Unwinding by eIF4G/4A/4B. To elucidate the molecular basis by which eIF4E stimulates IRES-mediated duplex unwinding, we examined whether eIF4E increases the rate of duplex unwinding

BIOCHEMISTRY

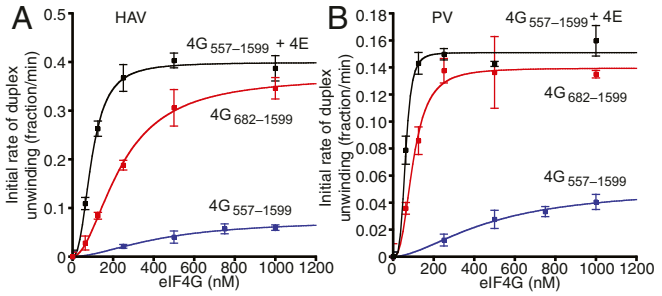

Fig. 3. eIF4E stabilizes eIF4G/4A/4B on the HAV and PV IRESs. (*A*) Initial rate of duplex unwinding on the HAV IRES with various concentrations of eIF4G$_{557–1,599}$ in the absence (blue) or presence of 1 μM eIF4E (black) or various concentrations of eIF4G$_{682–1,599}$ (red) with 1 μM eIF4A and eIF4B. (*B*) Initial rate of duplex unwinding on the PV IRES with various concentrations of eIF4G$_{557–1,599}$ in the absence (blue) or presence of 1 μM eIF4E (black) or various concentrations of eIF4G$_{682–1,599}$ (red) with 1 μM eIF4A and eIF4B. The initial rates of duplex unwinding are the mean of three independent experiments, and error bars indicate SEM.

and/or increases the apparent affinity of eIF4G/4A/4B to the HAV and PV IRESs. To this end, we measured duplex unwinding on both IRES constructs at fixed concentrations of eIF4A and eIF4B (1 μM each) and increasing concentrations of eIF4G$_{557–1,599}$ in the absence or presence of 1 μM eIF4E. In the presence of eIF4E, the apparent affinity ($K_{d,app}$) of the unwinding complex for the HAV IRES was increased by approximately fourfold [407 ± 55 nM (–4E) vs. 94 ± 3 nM (+4E)] (Fig. 3*A* and *SI Appendix*, Fig. S9*A* and Table S2). An even greater effect of eIF4E was observed on the PV IRES, where the $K_{d,app}$ of the unwinding complex for the PV IRES was increased by eightfold [477 ± 118 nM (–4E) vs. 61 ± 3 nM (+4E)] (Fig. 3*B* and *SI Appendix*, Fig. S9*B* and Table S2). Interestingly, the maximum rate of duplex unwinding at saturating concentrations of eIF4G$_{557–1,599}$ was also increased on both IRES constructs upon addition of eIF4E. The maximum rate of duplex unwinding on the HAV IRES was stimulated by fivefold, whereas that on the PV IRES was stimulated by threefold (Fig. 3 and *SI Appendix*, Table S2). This clearly indicates that eIF4E increases both the apparent affinity of the unwinding complex for these IRESs and stimulates the rate of eIF4A-dependent duplex unwinding.

We next wanted to determine how eIF4G cleavage by 2A^{pro} alters the interaction of the unwinding complex with the HAV and PV IRESs. Compared with eIF4G$_{557–1,599}$ in the absence of eIF4E, the apparent affinity of eIF4G$_{682–1,599}$ for the HAV and PV IRESs was increased by 1.7-fold (239 ± 10 nM) and 4.5-fold (98 ± 7 nM), respectively (Fig. 3 and *SI Appendix*, Fig. S9 and Table S2). However, with eIF4G$_{682–1,599}$, the maximum rate of duplex unwinding at saturation on both IRESs was essentially the same as eIF4E/eIF4G$_{557–1,599}$ (Fig. 3 and *SI Appendix*, Table S2). In contrast, a complex containing eIF4G$_{682–1,599}$ unwound a previously characterized non–IRES-containing duplex substrate at an appreciably slower rate at saturation compared with eIF4E/4G$_{557–1,599}$ (28) (*SI Appendix*, Fig. S10 and Table S2). This unexpected finding suggests that the PV and HAV IRESs bind and activate eIF4G$_{682–1,599}$ to stimulate the helicase activity of eIF4A.

eIF4E Enhances the Binding Affinity of eIF4G to dV of the PV IRES. To examine the molecular basis by which eIF4E increases the apparent affinity of eIF4G/4A/4B to the PV IRES, we directly measured the affinity of eIF4G for the PV IRES using a quantitative, fluorescent anisotropy equilibrium binding assay. Although the anisotropy assays were performed in a slightly different buffer than used in our unwinding assays, we did not observe a substantial change in affinity due to buffer composition (*SI Appendix*, Fig. S11*A*). Thus, we used optimized FP buffer for the binding experiments owing to the observed higher change in anisotropy signal (*SI Appendix*, Table S3). We found a modest K_d value for eIF4G$_{557–1,599}$ to PV dV-Fl of 276 ± 21 nM (Fig. 4). On the addition of eIF4E, the K_d value was reduced by a factor of 5, to 49 ± 2 nM (Fig. 4). This clearly demonstrates positive cooperativity between binding of eIF4G$_{557–1,599}$ and eIF4E on the PV IRES. To substantiate this finding, we found that a competition-binding assay using an unlabeled PV dV generated a similar affinity, albeit with a slightly more modest threefold reduction (*SI Appendix*, Fig. S12 and Table S3). Furthermore, filling the cap-binding pocket of eIF4E with m^{7}GTP had only a modest effect on the affinity of eIF4G$_{557–1,599}$ to PV dV-Fl (K_d = 96 ± 10; *SI Appendix*, Fig. S11*B* and Table S3).

We also examined whether a 2A^{pro} cleavage mimic of eIF4G can overcome the dependency of eIF4E for a high PV IRES binding affinity. Our data for eIF4G$_{682–1,599}$ show a K_d value of 75 ± 4 nM for PV dV-Fl (Fig. 4). This is very similar to the K_d value of 49 ± 2 nM for eIF4G$_{557–1,599}$ in the presence of eIF4E, indicating that the cleavage of eIF4G by 2A^{pro} substantially increases the affinity of eIF4G in the absence of eIF4E for the PV IRES. It should be noted that recombinant eIF4G$_{557–1,599}$ copurifies with an equimolar amount of eIF4A (28). Interestingly, the interaction of eIF4A with eIF4G$_{682–1,599}$ did not change the K_d of eIF4G$_{682–1,599}$ for PV dV-Fl (76 ± 10 nM; Fig. 4*B* and *SI Appendix*, Table S3). This indicates that eIF4A does not contribute to the interaction between eIF4G$_{682–1,599}$ and dV of the PV IRES. It should be noted that these binding experiments were carried out in the absence of ATP to prevent the duplex unwinding activity of eIF4A. Nevertheless, including AMP-PNP did not change the affinity of eIF4E/eIF4G$_{557–1,599}$ for PV dV-Fl (*SI Appendix*, Fig. S11*B* and Table S3). Taken together, our data support a model in which eIF4E binding to eIF4G enhances the affinity of eIF4F to the PV IRES before cleavage of eIF4G by 2A^{pro}. Subsequent cleavage of eIF4G generates a high-affinity binding state of eIF4G/4A that binds to the PV IRES independently of eIF4E.

Discussion

A typical feature of picornavirus translation is the requirement for a direct interaction between the viral IRES and eIF4G. This interaction plays two fundamental roles in directing IRES-mediated translation. First, eIF4G acts as a bridge between the IRES and the 43S preinitiation complex. Second, eIF4G functions to recruit eIF4A to restructure the IRES and enable ribosome recruitment. The eIF4E component of eIF4F is an additional regulator of IRES-mediated translation, but the mechanism by which it performs this function is unknown.

Our data show that eIF4E regulates picornavirus IRES-mediated translation by two distinct mechanisms. First, the binding of eIF4E to eIF4G increases the apparent affinity of the entire unwinding complex (including eIF4B) for the HAV and

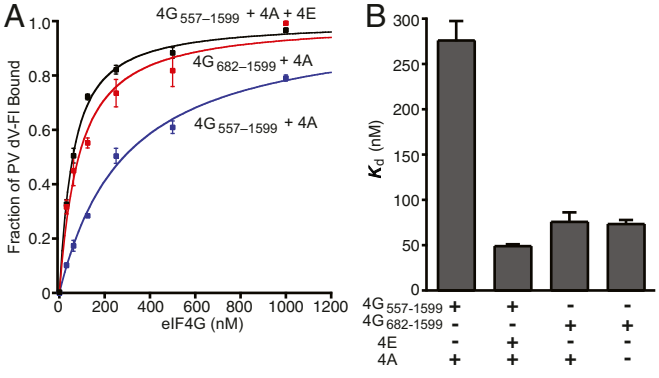

Fig. 4. eIF4E enhances binding of eIF4G to PV dV. (*A*) Equilibrium binding of PV dV-Fl RNA to eIF4G$_{557–1,599}$ + 4A (blue), eIF4G$_{557–1,599}$ + 4A + 4E (black), or eIF4G$_{682–1,599}$ + 4A (red). (*B*) Affinity of PV dV-Fl to the indicated eIF4G complexes. Each point represents the mean of three independent experiments, and error bars indicate SEM.

PV IRESs by fourfold and eightfold, respectively. Consistently, the equilibrium binding affinity of eIF4G for dV of the PV IRES is increased by fivefold in the presence of eIF4E. Second, our data show that eIF4E binding to eIF4G increases the rate of eIF4A-dependent duplex unwinding on the HAV and PV IRESs by fivefold and threefold, respectively (Fig. 3). These observations likely reflect the cap-independent function of eIF4E, which is to reverse the inhibition caused by an autoinhibitory domain in eIF4G (28). This suggests that the autoinhibitory domain in eIF4G regulates the interaction of eIF4F with picornavirus IRESs and the ability of eIF4A to restructure these IRESs to promote ribosome recruitment and translation. Although the HAV and PV IRESs do not share any obvious sequence or structural similarity, our data suggest that these diverse IRESs share apparent commonality in the way in which they bind and use the helicase activity of eIF4F to restructure their IRES domains. This may reflect a fundamental mechanism through which all viral RNAs interact with eIF4G, and we anticipate that future atomic resolution structural models will help determine this.

Curiously, the cap-binding pocket of eIF4E is required for efficient HAV IRES-mediated translation, yet we observed no defect in unwinding on the HAV IRES in the presence of m^7GTP cap analog, or with the use of an eIF4E W56L mutant in place of WT eIF4E (Fig. 2*D*). These findings suggest that the cap-binding ability of eIF4E is likely required for a step independent of eIF4F recruitment and IRES restructuring. It is important to note that the positive role of eIF4E on HAV IRES-mediated translation has not been verified during infection of cells with HAV. This verification has proven to be difficult because HAV barely grows in cell culture and accumulates attenuating mutations when passaged (30).

Two previous reports have shown that the addition of 4E-BP1 inhibits EMCV IRES-mediated translation in a nuclease-treated cell-free extract (3, 5). However, no titration was made to establish the extent of inhibition, and no model has been proposed to explain how 4E-BP1 could inhibit IRES-mediated translation. To precisely determine the extent to which eIF4E availability can regulate HAV, PV, and EMCV IRES-mediated viral translation, we used reporter genes containing these IRESs in a nuclease-treated cell-free extract. This system was used to avoid the complication of needing to account for the effects of competition between the IRES and endogenous mRNAs. In contrast to cap-dependent translation, the translation from these three IRES-containing reporters continued at an appreciably lower efficiency (~50%) in the absence of free eIF4E (Fig. 1 *C* and *D* and *SI Appendix*, Fig. S2*B*). This is consistent with a regulatory role of eIF4E in the translation of these different IRESs. To further strengthen these findings, we also monitored the translation of a PV replicon RNA that is competent for translation, viral polypeptide processing, and RNA replication (25). Consistent with the findings for the PV reporter, the addition of eIF4E and eIF4E W56L stimulated the rate of PV replicon translation by more than twofold compared with the addition of 4E-BP1 (Fig. 1*E*). Unfortunately, replication of PV was found to be inefficient in our lysate system, preventing us from determining whether the increased translation of the replicon also promotes viral replication. Nevertheless, these data show that eIF4E can have a positive effect on the translation of a PV replicon.

To understand the mechanism of eIF4G binding to the PV IRES during late viral infection, we investigated the interaction of eIF4G with this IRES following eIF4G cleavage. Our data show that the affinity (apparent and direct) of $eIF4G_{682–1,599}$ for the PV IRES is very similar to that of $eIF4G_{557–1,599}$ in the presence of eIF4E (*SI Appendix*, Table S2 and S3). Consistent with this, $eIF4G_{682–1,599}$ increased the rate of eIF4A-dependent duplex unwinding on the PV IRES to a similar level as $eIF4G_{557–1,599}$ in the presence of eIF4E (Fig. 3*B* and *SI Appendix*, Table S2). In contrast, $eIF4G_{682–1,599}$ could only partially stimulate eIF4A helicase activity on a non–IRES-containing duplex substrate compared with unwinding activation by $eIF4E/4G_{557–1,599}$ (28) (*SI Appendix*, Table S2). This unexpected result suggests that the PV IRES has an RNA-based activation domain that enables $eIF4G_{682–1,599}$ to fully stimulate the helicase activity of eIF4A. This activation mechanism appears to function only after eIF4G cleavage by $2A^{pro}$, while the eIF4E-dependent activation of eIF4G is required for maximum duplex unwinding before cleavage. Thus, our data reveal a plausible mechanism by which viral-mediated cleavage of eIF4G obviates the need for eIF4E during translation in the later stages of PV infection (Fig. 5).

Interestingly, eIF4E is required for rapid cleavage of eIF4G when using recombinant picornaviral proteases in cell-free extracts (26, 27). Our data strengthen this model by showing that a virally encoded $2A^{pro}$ is dependent on available eIF4E for cleaving eIF4G in a nuclease-treated lysate (Fig. 1*F* and *SI Appendix*, Fig. S6). However, we cannot rule out the possibility that some of the enhanced eIF4G cleavage that we observed might be due to the increased production of the $2A^{pro}$ in the presence of eIF4E. Nevertheless, since eIF4G cleavage is almost abolished in the presence of 4E-BP1, this is unlikely to completely explain this observation. It thus appears that eIF4E can positively function during PV infection by promoting PV translation and eIF4G cleavage by $2A^{pro}$ (Fig. 5). These positive effects of eIF4E on the PV lifecycle are puzzling given the fact that high eIF4E concentrations inhibit PV and EMCV translation and replication in the presence of endogenous mRNAs in cells and cell-free extracts (5). This is presumably due to competition between capped mRNAs and the viral IRES for free eIF4G. Thus, it will be important in the future to understand the degree to which the positive and negative effects of eIF4E can regulate picornavirus

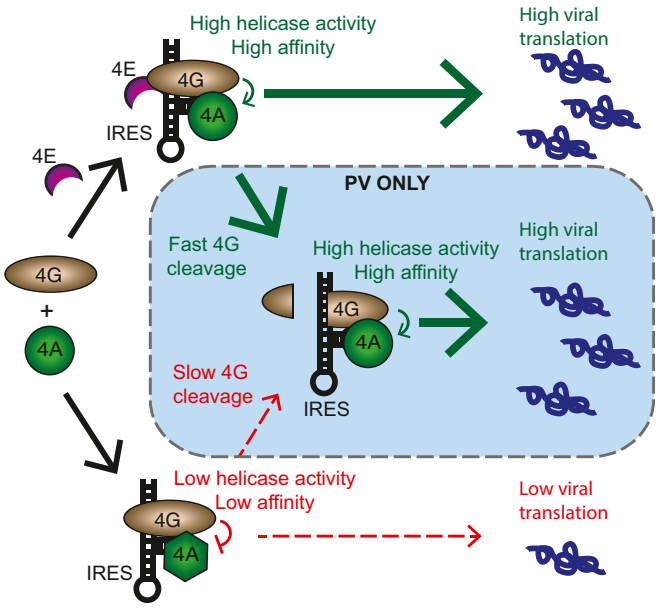

Fig. 5. Proposed mechanism by which eIF4E regulates IRES-mediated picornavirus translation. In the absence of eIF4E, eIF4G adopts a conformation with low eIF4A-stimulating activity and low affinity for the viral IRES. This results in low levels of viral translation (bottom pathway). In the presence of eIF4E, the conformation of eIF4G has high eIF4A helicase-stimulating activity and high affinity for the viral IRES. This results in high levels of viral translation (top pathway). Late during PV infection (dashed box), PV $2A^{pro}$ cleaves eIF4G, removing the N-terminal eIF4E-binding domain. The rate of eIF4G cleavage is much more efficient in the presence of eIF4E. The cleaved C-terminal domain of eIF4G has high eIF4A helicase-stimulating activity and high affinity on the PV RNA and results in high levels of viral translation.

translation in response to physiological conditions that alter the amount of competition between mRNAs. Interestingly, the production of infectious PV particles in single cells is very heterogeneous and generally independent of the number of viruses used in the infection (31). The precise molecular basis for this heterogeneity is not clear, but it is entirely possible that variation in eIF4E availability between cells could contribute to this phenomenon through its positive and negative effects on PV translation.

Materials and Methods

Purified Components. Protein expression, purification, and transcription protocols are described in detail in *SI Appendix, Materials and Methods*. Recombinant eIF4AI, eIF4B, eIF4E, eIF4E W56L, 4E-BP1, eIF4G$_{557–1,599}$, eIF4G$_{682–1,599}$, and Lb protease were prepared as described previously (20, 28, 32). Capped, HAV, PV, and EMCV RNAs for translation, HAV and PV RNAs for helicase assays, and PV dV RNA for fluorescence anisotropy assays were prepared as described previously (29) and in *SI Appendix, Materials and Methods*. A plasmid containing the PV-Luc replicon [prib(+)Luc-Wt] was a kind gift from Raul Andino (25). PV dV RNA for fluorescence anisotropy was 3′-labeled with fluorescein-5-thiosemicarbazide (Thermo Fisher Scientific) as described previously (33) and in *SI Appendix, SI Materials and Methods*.

In Vitro Translation. Translation assays were carried out in 50% nuclease-treated RRL (Promega) with the following final concentrations: 90 mM KOAc, 45 mM KCl, 2 mM Mg(OAc)$_2$, 0.5 U/μL rRNasin (Promega), a 20 μM amino acid mixture (– methionine), and a 20 μM amino acid mixture (– leucine). Translation reactions with the PV-Fluc reporter and PV-Luc replicon also included 12% HeLa extract. Proteins were incubated in lysate for 7–10 min at 30 °C in the absence of RNA. Then 5 μg/mL capped PV or EMCV, 100 μg/mL HAV, or 20 μg/mL PV-Luc replicon RNA was added, and the reactions were incubated for another 30 min at 30 °C. Firefly or *Renilla* luciferase assay substrate (Promega) was added, and luminescence was measured for 10 s with a VICTOR X5 multilabel plate reader (PerkinElmer). For PV-Luc replicon reactions, 1/10 volume was removed at each time point for measurement of luciferase production.

eIF4G Cleavage Assay. In vitro translation reactions were performed as described for the PV-Luc replicon but supplemented with 10% of a 10× rNTP/energy mix (10 mM ATP, 2.5 mM GTP, 2.5 mM CTP, 2.5 mM UTP, 300 mM creatine phosphate, 4 mg/mL creatine kinase, and 155 mM Hepes-KOH pH 7.4). At 4, 7, 9, and 12 h, a 1/5 volume of the reaction was analyzed by SDS/PAGE, and eIF4G was detected by immunoblotting using anti-eIF4G antibody (Proteintech; 15704-1-AP) as described in detail in *SI Appendix, Materials and Methods*.

Helicase Assay. Unwinding reactions were performed as described previously with minor modifications (29). Unwinding reactions were assayed with a Fluorolog-3 spectrofluorometer (Horiba), and data were analyzed as described previously (28, 29) and in *SI Appendix, Materials and Methods*.

Fluorescence Anisotropy Binding Assay. Fluorescence anisotropy was measured using a VICTOR X5 plate reader (PerkinElmer) and analyzed as described previously (33). Reactions containing 20 nM PV dV-Fl were incubated with varying concentrations of eIF4G in binding buffer (20 mM Hepes-KOH pH 7.5, 80 mM KCl, 2 mM $MgCl_2$, 1 mM DTT, and 0.1 mg/mL BSA) for 4 min at 37 °C, followed by 20 min at 25 °C.

ACKNOWLEDGMENTS. We thank John Hershey and members of the C.S.F. laboratory for their thoughtful comments and critical reading of the manuscript, Peter Sarnow for insightful discussions, Raul Andino for the prib(+)Luc-Wt plasmid, and Tim Skern for the L protease expression plasmid. This work was supported by National Institutes of Health Grant R01 GM092927 (to C.S.F.), an American Heart Association and Myocarditis Foundation predoctoral fellowship (to B.C.A.), and by start-up funds from University at Albany, State University of New York, and the University at Albany Faculty Research Awards Program (FRAP) (to G.F.).

1. Pelletier J, Sonenberg N (1988) Internal initiation of translation of eukaryotic mRNA directed by a sequence derived from poliovirus RNA. *Nature* 334:320–325.
2. Jang SK, et al. (1988) A segment of the 5′ nontranslated region of encephalomyocarditis virus RNA directs internal entry of ribosomes during in vitro translation. *J Virol* 62:2636–2643.
3. Pause A, et al. (1994) Insulin-dependent stimulation of protein synthesis by phosphorylation of a regulator of 5′-cap function. *Nature* 371:762–767.
4. Pestova TV, Shatsky IN, Hellen CU (1996) Functional dissection of eukaryotic initiation factor 4F: The 4A subunit and the central domain of the 4G subunit are sufficient to mediate internal entry of 43S preinitiation complexes. *Mol Cell Biol* 16:6870–6878.
5. Svitkin YV, et al. (2005) Eukaryotic translation initiation factor 4E availability controls the switch between cap-dependent and internal ribosomal entry site-mediated translation. *Mol Cell Biol* 25:10556–10565.
6. de Breyne S, Yu Y, Unbehaun A, Pestova TV, Hellen CU (2009) Direct functional interaction of initiation factor eIF4G with type 1 internal ribosomal entry sites. *Proc Natl Acad Sci USA* 106:9197–9202.
7. Kolupaeva VG, Lomakin IB, Pestova TV, Hellen CU (2003) Eukaryotic initiation factors 4G and 4A mediate conformational changes downstream of the initiation codon of the encephalomyocarditis virus internal ribosomal entry site. *Mol Cell Biol* 23:687–698.
8. Sweeney TR, Abaeva IS, Pestova TV, Hellen CU (2014) The mechanism of translation initiation on type 1 picornavirus IRESs. *EMBO J* 33:76–92.
9. Bordeleau ME, et al. (2006) Functional characterization of IRESs by an inhibitor of the RNA helicase eIF4A. *Nat Chem Biol* 2:213–220.
10. Redondo N, et al. (2012) Translation directed by hepatitis A virus IRES in the absence of active eIF4F complex and eIF2. *PLoS One* 7:e52065.
11. Etchison D, Milburn SC, Edery I, Sonenberg N, Hershey JW (1982) Inhibition of HeLa cell protein synthesis following poliovirus infection correlates with the proteolysis of a 220,000-Dalton polypeptide associated with eucaryotic initiation factor 3 and a cap binding protein complex. *J Biol Chem* 257:14806–14810.
12. Lamphear BJ, Kirchweger R, Skern T, Rhoads RE (1995) Mapping of functional domains in eukaryotic protein synthesis initiation factor 4G (eIF4G) with picornaviral proteases: Implications for cap-dependent and cap-independent translational initiation. *J Biol Chem* 270:21975–21983.
13. Gingras AC, Svitkin Y, Belsham GJ, Pause A, Sonenberg N (1996) Activation of the translational suppressor 4E-BP1 following infection with encephalomyocarditis virus and poliovirus. *Proc Natl Acad Sci USA* 93:5578–5583.
14. Sukarieh R, Sonenberg N, Pelletier J (2010) Nuclear assortment of eIF4E coincides with shut-off of host protein synthesis upon poliovirus infection. *J Gen Virol* 91:1224–1228.
15. Ali IK, McKendrick L, Morley SJ, Jackson RJ (2001) Activity of the hepatitis A virus IRES requires association between the cap-binding translation initiation factor (eIF4E) and eIF4G. *J Virol* 75:7854–7863.
16. Borman AM, Kean KM (1997) Intact eukaryotic initiation factor 4G is required for hepatitis A virus internal initiation of translation. *Virology* 237:129–136.
17. Borman AM, Michel YM, Kean KM (2001) Detailed analysis of the requirements of hepatitis A virus internal ribosome entry segment for the eukaryotic initiation factor complex eIF4F. *J Virol* 75:7864–7871.
18. Kozak M (1989) Context effects and inefficient initiation at non-AUG codons in eucaryotic cell-free translation systems. *Mol Cell Biol* 9:5073–5080.
19. Dorner AJ, et al. (1984) In vitro translation of poliovirus RNA: Utilization of internal initiation sites in reticulocyte lysate. *J Virol* 50:507–514.
20. Kirchweger R, et al. (1994) Foot-and-mouth disease virus leader proteinase: Purification of the Lb form and determination of its cleavage site on eIF-4 gamma. *J Virol* 68:5677–5684.
21. Borman AM, Bailly JL, Girard M, Kean KM (1995) Picornavirus internal ribosome entry segments: Comparison of translation efficiency and the requirements for optimal internal initiation of translation in vitro. *Nucleic Acids Res* 23:3656–3663.
22. Bergamini G, Preiss T, Hentze MW (2000) Picornavirus IRESs and the poly(A) tail jointly promote cap-independent translation in a mammalian cell-free system. *RNA* 6:1781–1790.
23. Dobrikova E, Florez P, Bradrick S, Gromeier M (2003) Activity of a type 1 picornavirus internal ribosomal entry site is determined by sequences within the 3′ nontranslated region. *Proc Natl Acad Sci USA* 100:15125–15130.
24. Svitkin YV, et al. (2001) Poly(A)-binding protein interaction with eIF4G stimulates picornavirus IRES-dependent translation. *RNA* 7:1743–1752.
25. Vogt DA, Andino R (2010) An RNA element at the 5′-end of the poliovirus genome functions as a general promoter for RNA synthesis. *PLoS Pathog* 6:e1000936.
26. Haghighat A, et al. (1996) The eIF4G-eIF4E complex is the target for direct cleavage by the rhinovirus 2A proteinase. *J Virol* 70:8444–8450.
27. Ohlmann T, Pain VM, Wood W, Rau M, Morley SJ (1997) The proteolytic cleavage of eukaryotic initiation factor (eIF) 4G is prevented by eIF4E binding protein (PHAS-I; 4E-BP1) in the reticulocyte lysate. *EMBO J* 16:844–855.
28. Feoktistova K, Tuvshintogs E, Do A, Fraser CS (2013) Human eIF4E promotes mRNA restructuring by stimulating eIF4A helicase activity. *Proc Natl Acad Sci USA* 110:13339–13344.
29. Özeş AR, Feoktistova K, Avanzino BC, Baldwin EP, Fraser CS (2014) Real-time fluorescence assays to monitor duplex unwinding and ATPase activities of helicases. *Nat Protoc* 9:1645–1661.
30. Konduru K, Kaplan GG (2006) Stable growth of wild-type hepatitis A virus in cell culture. *J Virol* 80:1352–1360.
31. Schulte MB, Andino R (2014) Single-cell analysis uncovers extensive biological noise in poliovirus replication. *J Virol* 88:6205–6212.
32. Özeş AR, Feoktistova K, Avanzino BC, Fraser CS (2011) Duplex unwinding and ATPase activities of the DEAD-box helicase eIF4A are coupled by eIF4G and eIF4B. *J Mol Biol* 412:674–687.
33. Sokabe M, Fraser CS (2017) A helicase-independent activity of eIF4A in promoting mRNA recruitment to the human ribosome. *Proc Natl Acad Sci USA* 114:6304–6309.